ELSEVIER

Polymer 40 (1999) 5865–5871

polymer

Vapor–liquid equilibria for binary solutions of polyisobutylene in C_6 through C_9 *n*-alkanes

John G. Lieu[a], John M. Prausnitz[a,b,*]

[a]*Chemical Engineering Department, University of California, Berkeley, CA, USA*
[b]*Chemical Sciences Division, Lawrence Berkeley National Laboratory, Berkeley, CA 94720, USA*

Received 1 September 1998; received in revised form 6 November 1998; accepted 8 November 1998

Abstract

Vapor–liquid equilibria for binary solutions of polyisobutylene in C_6 through C_9 *n*-alkanes were obtained at 65°C. Using a classic gravimetric-sorption method, the amount of solvent absorbed by polyisobutylene was measured as a function of solvent vapor pressure. The data were interpreted by the Flory–Huggins theory and the Prigogine–Flory–Patterson theory. © 1999 Elsevier Science Ltd. All rights reserved.

Keywords: Vapor–liquid-equilibrium; Polyisobutylene; Flory–Huggins theory

1. Introduction

Vapor–liquid-equilibrium (VLE) data for polymer solutions are useful for a variety of applications including surface acoustic-wave sensors, polymer devolatilization, polymeric membrane-separation processes, pervaporation, and vapor-phase photografting [1–6]. Efficient design of such processes requires characterizing VLE behavior of polymer solutions through experimental data or molecular-thermodynamic models.

Modeling polymer-solution properties is traditionally done by lattice theory or by equation-of-state theory; the Flory–Huggins lattice theory [7] and the Prigogine–Flory–Patterson equation-of-state theory [8–11] provide classical examples. In general, an equation-of-state theory gives a more complete and accurate description of real polymer solutions than the lattice theory. For example, the excess volume upon mixing is accessible through an equation-of-state model but not through an incompressible lattice model. However, while the Flory–Huggins lattice theory requires only one adjustable interaction parameter, the Prigogine–Flory–Patterson theory requires an adjustable interaction parameter in addition to three pure-component parameters for the solvent and for the polymer.

This work reports vapor–liquid-equilibrium data for binary solutions of polyisobutylene (PIB) in C_6 through C_9 *n*-alkanes. Data are interpreted with the Flory–Huggins theory and with the Prigogine–Flory–Patterson theory.

2. Experimental

2.1. Materials

Solvents were degassed with a standard freeze-thaw procedure described by Panayiotou and Vera [12] and used without further purification.

The PIB sample was a white, rubbery solid with a glass-transition temperature of about 29°C. The viscosity-average molecular weight was in the range of 4.2×10^6–5.2×10^6. An average value of 4.7×10^6 was assumed in our calculations.

Table 1 gives the properties of solvents and PIB.

2.2. Apparatus

Vapor–liquid-equilibrium data were collected using a gravimetric-sorption method previously described by several authors (see for example, Gupta and Prausnitz [13]). Fig. 1 shows a schematic diagram of the apparatus. The entire system is submerged in an isothermal water bath maintained at ±0.1°C.

Each glass chamber contains one aluminum pan suspended from a quartz spring (Ruska Instruments Corp., Houston, TX). The calibrated springs have a sensitivity of about 1 mg/mm and a maximum load of 250 mg. Within this

* Corresponding author. Tel.: + 1 510 642 3592; fax: + 1 510 642 4778.

0032-3861/99/$ - see front matter © 1999 Elsevier Science Ltd. All rights reserved.
PII: S0032-3861(98)00794-0

Table 1
Solvent and polymer properties

Substance	Supplier	Lot number	Purity
n-hexane	Aldrich Chemical Co., Inc.	13004CR	99 + %
n-heptane	Sigma-Aldrich	06438LQ	99 + %
n-octane	Aldrich Chemical Co., Inc.	JR01557HR	99 + %
n-nonane	Aldrich Chemical Co., Inc.	ER10504PQ	99%
PIB	Aldrich Chemical Co., Inc.	AF03243TZ	

range, the elongation of each spring is linear with respect to the change in mass.

A cathetometer (Gaertner Scientific Corp., Chicago) is used to measure the extension of the springs and the mercury levels of the manometer.

2.3. Experimental procedure

Polymer samples of known mass (20–25 mg) are placed into previously weighed aluminum pans. The system is then vacuum-dried for 12–24 h to remove residual moisture and solvent. After obtaining the mass of dry polymer, solvent is introduced by opening and then closing the valve between the solvent flask and the evacuated glass chambers.

The system is allowed to equilibrate anywhere from 12 h to a few days after each solvent injection. Equilibrium is assumed when measurements in spring length do not change more than $\pm$ 0.03 mm over a 12-h period.

As the polymer is nonvolatile, the total pressure is equal to the vapor pressure of solvent above the polymer solution. Also, as the experimental pressures are low (less than 0.9 bar), the solvent vapor is considered to be an ideal gas. Solvent activity a_1 is given by the ratio of the measured pressure to the pure-solvent saturation pressure at the system temperature.

The vernier scale on the cathetometer allows measurements to be made to the nearest 0.01 mm; therefore,

Table 2
Vapor–liquid-equilibrium data for polyisobutylene in *n*-alkanes at 65°C[w_1 = solvent weight fraction in the liquid phase; Φ = solvent segment fraction in the liquid phase; $a_1 = P/P_1^{sat}$ = solvent activity; P = vapor pressure in torr; P_1^{sat} = pure-solvent saturation pressure (calculated from equations suggested by Daubert and Danner [26]) in torr]

Solvent: *n*-Hexane; $P_1^{sat} = 671$ torr			Solvent: *n*-Heptane; $P_1^{sat} = 255$ torr		
w_1	Φ_1	a_1	w_1	Φ_1	a_1
0.011	0.016	0.117	0.017	0.023	0.122
0.030	0.043	0.232	0.040	0.055	0.243
0.060	0.085	0.343	0.067	0.091	0.367
0.087	0.122	0.464	0.097	0.130	0.487
0.121	0.167	0.580	0.135	0.178	0.604
0.162	0.219	0.694	0.179	0.232	0.720
0.217	0.287	0.792	0.237	0.301	0.829
0.292	0.374	0.890	0.292	0.364	0.904
0.401	0.493	0.967	0.350	0.428	0.972
			0.451	0.533	1.000
Solvent: *n*-Octane; $P_1^{sat} = 96$ torr			Solvent: *n*-Nonane; $P_1^{sat} = 37$ torr		
w_1	Φ_1	a_1	w_1	Φ_1	a_1
0.021	0.028	0.171	0.021	0.027	0.137
0.040	0.053	0.276	0.053	0.068	0.320
0.065	0.085	0.427	0.073	0.094	0.453
0.091	0.119	0.550	0.104	0.132	0.591
0.122	0.157	0.670	0.134	0.169	0.720
0.156	0.199	0.777	0.167	0.208	0.863
0.199	0.250	0.879			

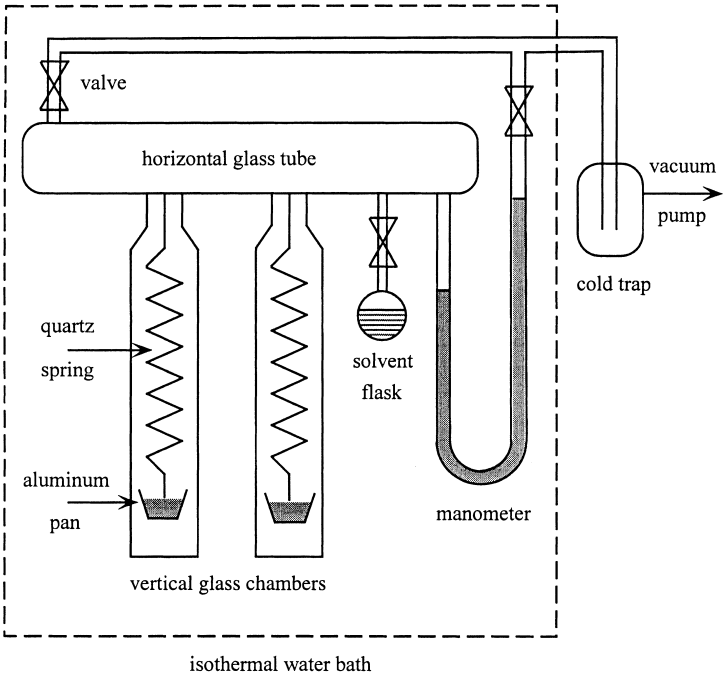

Fig. 1. Experimental apparatus for vapor–liquid equilibrium measurements.

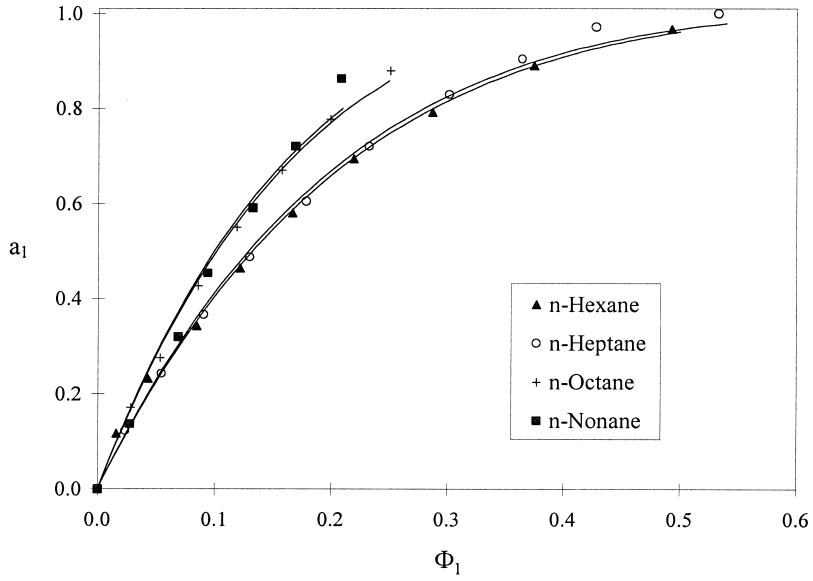

Fig. 2. Calculated solvent activities (solid lines) for binary solutions of PIB in *n*-alkanes at 65°C; data fitted with the Flory–Huggins equation; points are experimental.

pressure and mass readings have a precision of 0.02 torr and 0.02 mg, respectively. Uncertainty in solvent activity is less than 1% for the pressures used here. Solvent weight fraction w_1 uncertainty is less than 1% above $w_1 = 0.1$ and 1%–10% below $w_1 = 0.1$. Reliability of the apparatus and experimental procedure were established by reproducing the published experimental vapor–liquid-equilibrium data for polystyrene in chloroform at 50°C [14].

3. Results and discussion

Table 2 presents vapor–liquid-equilibrium data for PIB in C_6 through C_9 *n*-alkanes.

The data were fitted using the Flory–Huggins lattice theory [7] and the Prigogine–Flory–Patterson equation-of-state theory [8–11].

3.1. Flory–Huggins theory

The activity of the solvent is given by

$$\ln a_1 = \ln \Phi_1 + \left(1 - \frac{r_1}{r_2}\right)\Phi_2 + \chi_{FH}\Phi_2^2. \quad (1)$$

Solvent and polymer segment fractions, Φ_1 and Φ_2, are defined by

$$\Phi_2 = 1 - \Phi_1 = \frac{r_2 N_2}{r_1 N_1 + r_2 N_2}, \quad (2)$$

where N_1 and N_2 are the number of molecules and r_1 and r_2 the number of segments per molecule of solvent and polymer, respectively. We set r_1 equal to unity and calculate r_2 by

$$r_2 = \frac{M_2}{M_1}\frac{\rho_1}{\rho_2} = \frac{\text{molar volume of polymer}}{\text{molar volume of solvent}}, \quad (3)$$

where M_1 and M_2 are molecular weights, and ρ_1 and ρ_2 are mass densities of solvent and polymer, respectively. The dimensionless Flory–Huggins parameter χ_{FH} characterizes the solvent–polymer interaction energy; the lower this parameter, the stronger the attraction between solvent and polymer. Fig. 2 shows that our vapor–liquid-equilibrium data are fit reasonably well by adjusting χ_{FH}. Table 3 gives the fitted χ_{FH} values and indicates that the solvent power of *n*-alkanes decreases (increasing χ_{FH}) with rising alkane carbon number.

Table 3
Flory–Huggins interaction parameter for polyisobutylene in *n*-alkanes at 65°C

n-Alkane	χ_{FH}
C_6	0.612
C_7	0.637
C_8	0.860
C_9	0.877

3.2. Prigogine–Flory–Patterson theory

The Prigogine–Flory–Patterson theory gives a reduced equation of state

$$\frac{\tilde{P}\tilde{\nu}}{\tilde{T}} = \frac{\tilde{\nu}^{1/3}}{\tilde{\nu}^{1/3} - 1} - \frac{1}{\tilde{\nu}\tilde{T}}, \quad (4)$$

where temperature T, pressure P, and specific volume ν, are reduced, respectively, by characteristic parameters T^*, P^*, and ν^* such that

$$\tilde{T} = \frac{T}{T^*}, \quad (5)$$

Table 4
Pure-component parameters for the Prigogine–Flory–Patterson theory (Parameters for polyisobutylene estimated from Eichinger and Flory [24], ν_1 and P_1* for *n*-alkanes estimated from Orwoll and Flory [27], T_1* and ν_1* for *n*-alkanes estimated from Flory et al. [28] s_2/s_1 calculated from structural data following Flory et al. [17])

Substance	ν_i (cm^3/g)	ν_i* (cm^3/g)	T_i* (K)	P_i* (cal/cm^3)	s_2/s_1
n-hexane	1.620	1.162	4510	97	0.549
n-heptane	1.551	1.144	4757	99	0.565
n-octane	1.503	1.126	4946	100	0.577
n-nonane	1.465	1.115	5096	102	0.587
PIB	1.114	0.952	7820	105	

$$\tilde{\nu} = \frac{\nu}{\nu^*}, \tag{6}$$

$$\tilde{P} = \frac{P}{P^*}. \tag{7}$$

A binary mixture requires six pure-component parameters: T_1*, T_2*, ν_1*, ν_2*, P_1*, and P_2*. For pure solvents and polymers, these parameters are found from volumetric data. Table 4 shows pure-component parameters for PIB and *n*-alkanes; we define T* in Kelvin, ν* in cm^3/g, and P* in cal/cm^3.

For the mixture, T* and P* depend on the composition according to

$$T^* = \frac{P^*}{(P_1^*/T_1^*)\Phi_1^* + (P_2^*/T_2^*)\Phi_2^*}, \tag{8}$$

and

$$P^* = P_1^*\Phi_1^* + P_2^*\Phi_2^* - \Phi_1^*\theta_2 X_{12}, \tag{9}$$

where Φ_1*,Φ_2*, θ_1, and θ_2 are, respectively the segment fractions and surface fractions of the solvent and polymer and given by

$$\Phi_2^* = 1 - \Phi_1^* = \frac{m_2\nu_2^*}{m_1\nu_1^* + m_2\nu_2^*}, \tag{10}$$

and

$$\theta_2 = 1 - \theta_1 = \frac{(s_2/s_1)\Phi_2^*}{\Phi_1^* + (s_2/s_1)\Phi_2^*}, \tag{11}$$

where m_1 and m_2 are the masses of solvent and polymer, respectively. As the solvent and polymer segments are chosen to have the same core volume, the segment-surface ratio s_2/s_1 is the ratio of surfaces per unit core volume, estimated from structural data, as tabulated, for example, by Bondi [15]. However, Flory and Höcker [16] note that using the group surface-area increments by Bondi overestimates the available surface area of polymers because it ignores the shielding of constituent groups by intramolecular contacts between near-neighbors in the polymer chain. Thus, we follow Flory et al. [17] and calculate s_2/s_1 from crystallographic data as follows. We consider *n*-alkanes to be right cylinders with length $L_1 = 1.19n + 1.32$Å, mean radius $R_1 = 2.49$Å, molecular surface area A_1, and core molar volume V_1*. Similarly, we consider PIB to be a right cylinder divided into repeat units, with length $L_u = 2.325$Å, radius $R_u = 3.48$Å, molecular surface area A_u, and core molar volume V_u*. The ratio s_2/s_1 is then calculated by

$$\frac{s_2}{s_1} = \frac{A_u}{A_1}\frac{V_1^*}{V_u^*}. \tag{12}$$

Molecular surface areas are defined by

$$A_1 = 2\pi R_1 L_1 + 2\pi R_1^2, \tag{13}$$

and

$$A_u = 2\pi R_u L_u, \tag{14}$$

and core molar volumes are defined by

$$V_1^* = \pi R_1^2 L_1 N_{av} \tag{15}$$

and

$$V_u^* = \pi R_u^2 L_u N_{av} \tag{16}$$

where N_{av} is Avogadro's number.

For the mixture, the reduced volume $\tilde{\nu}$ can be conveniently determined by following the procedure of Flory et al. [18]. First, we define an ideal reduced volume

$$\tilde{\nu}^0 = \Phi_1^*\tilde{\nu}_1 + \Phi_2^*\tilde{\nu}_2, \tag{17}$$

where

$$\tilde{\nu}_1 = \frac{\nu_1}{\nu_1^*}, \tag{18}$$

and

$$\tilde{\nu}_2 = \frac{\nu_2}{\nu_2^*}. \tag{19}$$

The reduced volume of the real mixture is given by

$$\tilde{\nu} = \tilde{\nu}^0 + \tilde{\nu}^E. \tag{20}$$

The excess volume is calculated from

$$\tilde{\nu}^E = \left(\frac{\partial\tilde{\nu}}{\partial\tilde{T}}\right)(\tilde{T} - \tilde{T}^0) = \frac{3(\tilde{\nu}^0)^{7/3}}{4 - 3(\tilde{\nu}^0)^{1/3}}(\tilde{T} - \tilde{T}^0), \tag{21}$$

where the reduced temperature corresponding to $\tilde{\nu}^0$ is found by rearranging Eq. (4) for $P = 0$, such that

$$\tilde{T}^0 = \frac{(\tilde{\nu}^0)^{1/3} - 1}{(\tilde{\nu}^0)^{4/3}}. \tag{22}$$

Eq. (21) provides an excellent approximation for polymer solutions at low or moderate pressures where pressure has a negligible effect on thermodynamic properties. The solvent

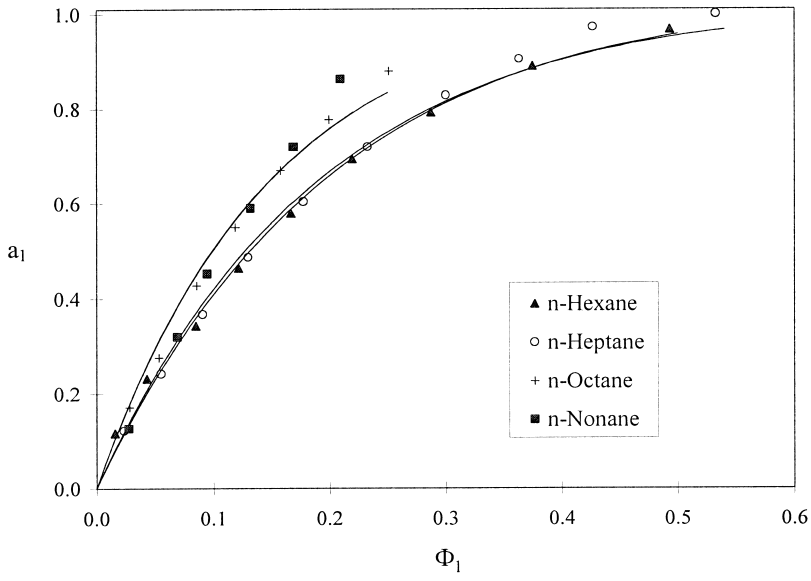

Fig. 3. Calculated solvent activities (solid lines) for binary solutions of PIB in *n*-alkanes at 65°C; data fitted with the Prigogine–Flory–Patterson equation of state; points are experimental.

activity is then given by

$$\ln a_1 = \ln \Phi_1^* + \left(1 - \frac{r_1}{r_2}\right)\Phi_2^* + \frac{P_1^* M_1 \nu_1^*}{RT}\left[3\tilde{T}_1 ln\frac{\tilde{\nu}_1^{1/3} - 1}{\tilde{\nu}^{1/3} - 1} + \left(\frac{1}{\tilde{\nu}_1} - \frac{1}{\tilde{\nu}}\right)\right] + \frac{M_1 \nu_1^*}{RT}\left(\frac{X_{12}}{\tilde{\nu}}\right)\theta_2^2 \quad (23)$$

where M_1 is the solvent molecular weight and R is the universal gas constant. The interchange-interaction parameter, X_{12}, measures the energy change upon formation of a solvent–polymer segment contact from a solvent–solvent and a polymer segment–polymer segment contact. The lower the value of X_{12}, the stronger the attraction between solvent and polymer.

Fig. 3 shows the solvent-activity data fitted with the Prigogine–Flory–Patterson theory. As shown in Table 5, X_{12} increases from C_6 to C_8, but surprisingly decreases from C_8 to C_9. Similar results for X_{12}, however, were reported by Kasprzycka-Guttman et al. [19,20] who measured heats of mixing for γ-picoline in C_6 through C_{10} *n*-alkanes and found that X_{12} is not monotonic with alkane carbon number.

Table 5
Interchange-interaction parameter X_{12} fitted to solvent-activity data

n-Alkane	X_{12} (cal/cm^3)
C_6	2.00
C_7	2.21
C_8	3.69
C_9	3.36

A significant advantage of the Prigogine–Flory–Patterson theory is its ability to account for negative enthalpies of mixing without necessarily assigning negative interchange energies. Instead, observed negative enthalpies of mixing are accounted for with equation-of-state contributions, e.g. negative excess volumes upon mixing. Delmas et al. [21] obtained enthalpy-of-mixing data for mixtures of PIB and *n*-alkanes and found them to be negative and to decrease in magnitude from C_6 to C_{10} *n*-alkanes. Using the Prigogine–Flory–Patterson theory, Flory et al. [17] calculated X_{12} from these enthalpy-of-mixing data and showed that X_{12} is positive and decreases with rising alkane carbon number, as shown in Table 6. For mixtures of nonpolar molecules, such as PIB and *n*-alkanes, the interchange energy should be small and positive. Further, it is expected that the interchange energy decreases with alkane carbon number; as the carbon number $\rightarrow \infty$, the contact energy for mixing polymethylene segments and PIB should decline to a small value.

As Eichinger and Flory [22] pointed out, however, X_{12} found from enthalpy-of-mixing data does not agree well with X_{12} found from solvent-activity data. Therefore, we follow the proposed extension of the Prigogine–Flory–Patterson theory by Orwoll and Flory [23] and express solvent activity by

$$\ln a_1 = \ln \Phi_1^* + \left(1 - \frac{r_1}{r_2}\right)\Phi_2^* + \frac{P_1^* M_1 \nu_1^*}{RT}\left[3\tilde{T}_1 ln\frac{\tilde{\nu}_1^{1/3} - 1}{\tilde{\nu}^{1/3} - 1} + \left(\frac{1}{\tilde{\nu}_1} - \frac{1}{\tilde{\nu}}\right)\right] + \frac{M_1 \nu_1^*}{RT}\left(\frac{X_{12}}{\tilde{\nu}} - TQ_{12}\right)\theta_2^2, \quad (24)$$

Table 6
Flory's X_{12} from enthalpy-of-mixing data and fitted TQ_{12} using an extended Prigogine–Flory–Patterson theory; $T = 338.15$ K

n-alkane	X_{12} (cal/cm^3)	TQ_{12} (cal/cm^3)
C_6	1.75	−0.205
C_7	1.28	−0.770
C_8	1.05	−2.191
C_9	0.91[a]	−2.045

[a] Estimated.

where parameter Q_{12} accounts for the interaction entropy. Fig. 4 shows that upon introducing Q_{12}, vapor–liquid-equilibrium data measured here can be fitted using Flory's X_{12} values obtained from enthalpy-of-mixing data. Table 6 lists fitted TQ_{12}.

A deficiency of the Prigogine–Flory–Patterson theory may follow from overestimating the magnitude of $\tilde{\nu}^E$, thereby underestimating X_{12}. A larger negative $\tilde{\nu}^E$ causes X_{12} to become less positive. Table 7 shows that the Prigogine–Flory–Patterson theory significantly overestimates the magnitude of $\tilde{\nu}^E$ in mixtures of PIB and *n*-alkanes investigated by Flory et al. [17].

A comparison of results shown in Figs. 2–4 indicates that our data are not fit better with the Prigogine–Flory–Patterson theory than with the Flory–Huggins theory. Application of the Prigogine–Flory–Patterson theory may be less successful than hoped because pure-component parameters for PIB vary with molecular weight. We used pure-component parameters reported by Eichinger and Flory [24] based on a viscosity-average molecular weight of ca. 4×10^4, whereas the molecular weight of the sample used here is ca. 4.7×10^6, two orders of magnitude larger. Although theory predicts that VLE behavior should converge at high polymer molecular weights, experimental data do not always agree with this prediction. For example, Wang et al. [25] showed that diethyl-ether solubility significantly depended on polymer molecular weight in high-molecular-weight poly(butyl methacrylate).

Table 7
Calculated and observed $\tilde{\nu}^E$ for binary solutions of polyisobutylene in *n*-alkanes investigated by Flory et al. [17]

n-Alkane	$\tilde{\nu}^E_{observed} \times 100$	$\tilde{\nu}^E_{calculated} \times 100$	% Overestimation[a]
C_5	−1.583	−1.920	21.3
C_6	−1.043	−1.214	16.4
	−1.053	−1.191	13.2
	−0.995	−1.066	7.1
C_7	−0.749	−0.902	20.3
C_8	−0.578	−0.661	14.4
	−0.582	−0.653	12.3
	−0.564	−0.624	10.6
C_{10}	−0.342	−0.399	16.6
	−0.349	−0.396	13.4
	−0.330	−0.428	30.0
C_{16}	−0.092	−0.131	42.9
	−0.095	−0.131	37.5
	−0.092	−0.118	28.2

[a] $\left(\frac{\tilde{\nu}^E_{observed} - \tilde{\nu}^E_{calculated}}{\tilde{\nu}^E_{observed}}\right) \times 100\%$.

4. Conclusions

New vapor–liquid-equilibrium data for PIB in *n*-alkanes indicate that alkane solubility decreases as alkane carbon number rises. Data were reduced using the Flory–Huggins theory and the Prigogine–Flory–Patterson theory. Both

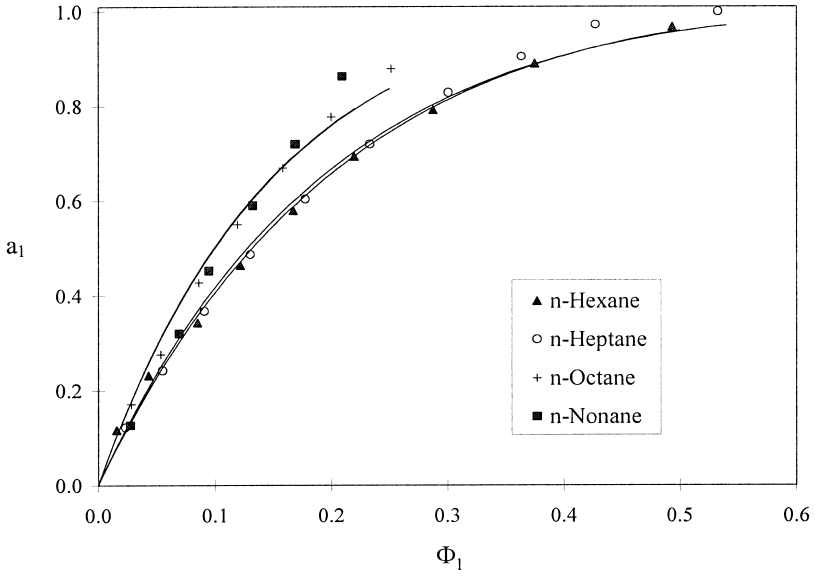

Fig. 4. Calculated solvent activities (solid lines) for binary solutions of PIB in *n*-alkanes at 65°C; data fitted with an extended Prigogine–Flory–Patterson equation of state; points are experimental.

theories give a fair representation of the data. An extended Prigogine–Flory–Patterson theory correlates the vapor–liquid-equilibrium data using Flory's X_{12} parameters calculated from enthalpy-of-mixing data.

Acknowledgements

This work was supported by the Director, Office of Energy Research, Office of Basic Energy Sciences, Chemical Sciences Division of the U.S. Department of Energy under contract No. DE-AC03-76SF0098, and by the Donors of the Petroleum Research Fund administered by the American Chemical Society. The authors are grateful to John O. Tanbonliong and Cristina Mio for construction of experimental apparatus and helpful comments.

References

[1] Ballantine DS, Wohltjen H. Anal Chem 1989;61:704A.
[2] High MS, Danner RP. Fluid Phase Equilib 1990;55:1.
[3] Baker RW, Yoshioka N, Mohr JM, Khan AJ. J Membr Sci 1987;31:259.
[4] Matsumoto K, Ishii K, Kuroda T, Inoue K, Iwama A. Polym J 1991;23:491.
[5] Maeda Y, Tsuyumoto M, Karakane H, Tsugaya H. Polym J 1991;23:501.
[6] Kubota H, Yoshino N, Ogiwara Y. J Appl Polym Sci 1990;39:1231.
[7] Flory PJ. Principles of polymer chemistry. New York: Cornell University Press, 1953.
[8] Flory PJ. Disc Faraday Soc 1970;49:7.
[9] Patterson D. Macromolecules 1969;2:672.
[10] Patterson D, Delmas G. Disc Faraday Soc 1970;49:98.
[11] Prigogine I. The molecular theory of solutions. Amsterdam: North-Holland Publishing Company, 1957.
[12] Panayiotou C, Vera JH. Polym J 1984;16:89.
[13] Gupta RB, Prausnitz JM. J Chem Eng Data 1995;40:784.
[14] Bawn CEH, Wajid MA. Trans Faraday Soc 1956;52:1658.
[15] Bondi A. Physical properties of molecular crystals, liquids and glasses. New York: Wiley, 1968.
[16] Flory PJ, Höcker H. Trans Faraday Soc 1971;67:2258.
[17] Flory PJ, Ellenson JL, Eichinger BE. Macromolecules 1968;1:279.
[18] Flory PJ, Orwoll RA, Vrij A. J Am Chem Soc 1964;86:3515.
[19] Kasprzycka-Guttman T, Wilczura H. Thermochim Acta 1991;184:321.
[20] Kasprzycka-Guttman T, Kurcińska H. Thermochim Acta 1990;173:63.
[21] Delmas G, Patterson D, Somcynsky T. J Polym Sci 1962;57:79.
[22] Eichinger BE, Flory PJ. Trans Faraday Soc 1968;64:2035.
[23] Orwoll RA, Flory PJ. J Am Chem Soc 1967;89:6822.
[24] Eichinger BE, Flory PJ. Macromolecules 1968;1:285.
[25] Wang K, Hu Y, Wu DT. J Chem Eng Data 1994;39:916.
[26] Daubert TE, Danner RP. Physical and thermodynamic properties of pure chemicals: data compilation. New York: Hemisphere Pub Corp, 1989.
[27] Orwoll RA, Flory PJ. J Am Chem Soc 1967;89:6814.
[28] Flory PJ, Orwoll RA, Vrij A. J Am Chem Soc 1964;86:3507.